ELSEVIER

Available online at www.sciencedirect.com

SCIENCE DIRECT®

Biochimica et Biophysica Acta 1657 (2004) 33–46

BIOCHIMICA ET BIOPHYSICA ACTA
BBA

www.bba-direct.com

Correlation between lifetime heterogeneity and kinetics heterogeneity during chlorophyll fluorescence induction in leaves: 1. Mono-frequency phase and modulation analysis reveals a conformational change of a PSII pigment complex during the IP thermal phase

Nicolae Moise*, Ismaël Moya

Laboratoire pour l'Utilisation du Rayonnement Electromagnétique, Centre Universitaire Paris-Sud, Bat. 209D, 91898 Orsay, France

Received 28 November 2003; received in revised form 17 March 2004; accepted 1 April 2004
Available online 20 April 2004

Abstract

The relationship between the fluorescence lifetime (τ) and yield (Φ) obtained in phase and modulation fluorometry at 54 MHz during the chlorophyll fluorescence induction in dark-adapted leaves under low actinic light has been investigated. Three typical phases have been identified: (i) linear during the OI photochemical rise, (ii) convex curvature during the subsequent IP thermal rise, and (iii) linear during the PS slow decay. A similar relationship has been obtained in the fluorescence induction for the fluorescence yield measured at 685 nm plotted versus the fluorescence yield measured at 735 nm. A spectrally resolved analysis shows that the curvature of the $\tau-\Phi$ relationship is not due to chlorophyll fluorescence reabsorption effects. Several other hypotheses are discussed and we conclude that the curvature of the $\tau-\Phi$ relationship is due to a variable and transitory nonphotochemical quenching. We tentatively propose that this quenching results from a conformational change of a pigment–protein complex of Photosystem II core antenna during the IP phase and could explain both spectral and temporal transitory changes of the fluorescence. A variable blue shift of the 685 nm peak of the fluorescence spectrum during the IP phase has been observed, supporting this hypothesis.

Keywords: Chlorophyll *a* fluorescence induction; Fluorescence lifetime; $\tau-\Phi$ relationship; Photochemical and thermal phase; Nonphotochemical quenching; Pigment–protein complex conformational change

1. Introduction

The response of a leaf submitted to a dark-to-light transition or to a change in light intensity displays a complex polyphasic time course of the chlorophyll (Chl) *a* fluorescence yield called "fluorescence induction curve" or "fluorescence transient" [1–3]. A fast increase of the fluorescence in the first second of illumination is followed by a slow decrease in a time range of minutes. Several interpretations of the different phases of the fluorescence induction have been given [4–6], although not all of them are fully elucidated [7,8].

Under natural light conditions in the field, the photosynthetic apparatus normally operates below saturating light intensity. Using low and moderate incident light, a dark-adapted leaf displays the well-known two-step fluorescence rise, denoted OIP, sometimes with a dip (D) preceding the IP rise. It is a well accepted fact that the fast OI phase of the fluorescence induction is a photochemical phase, since it reflects only the reduction of the primary electron acceptor Q_A [3,9] mainly from Q_B-non-reducing Photosystem II (PSII) reaction centers [3,10,11].

Abbreviations: Chl, chlorophyll; OIDPSMT, nomenclature for Chl *a* fluorescence induction; OI, photochemical phase; IP, thermal phase; F_o, minimal fluorescence level; F_m, maximal fluorescence level in dark-adapted leaves under saturating actinic light; F_p, fluorescence peak in dark-adapted leaves under low actinic light; F_s, steady-state fluorescence level; F_v, variable fluorescence, (F_m-F_o or F_p-F_o); DCMU, 3-(3,4-dichlorophenyl)-1,1-dimethylurea; PSI, Photosystem I; PSII, Photosystem II; PQ, plastoquinone; Q_A, primary quinone electron acceptor of PSII; Q_B, second quinone electron acceptor of PSII; LHCII, light-harvesting complex of PSII; NPQ, nonphotochemical quenching; FWHM, full width at half maximum; PMF, phase and modulation fluorometry; TCSPC, time-correlated single photon counting

* Corresponding author. Tel.: +33-1-6446-8054; fax: +33-1-6446-8007.

E-mail address: nicolae.moise@lure.u-psud.fr (N. Moise).

0005-2728/$ - see front matter © 2004 Elsevier B.V. All rights reserved.
doi:10.1016/j.bbabio.2004.04.001

The subsequent fluorescence rise, from I to P, is mainly explained by the development of a Q_A reduction/oxidation quasi-stationary state. It was also found that a gradual reduction of the plastoquinone (PQ) pool occurs during the IP phase with a maximum at the P point [1,9,11,12]. This process is accompanied by the gradual removal of the nonphotochemical quenching (NPQ) due to oxidized PQ pool [13]. Under low light illumination and in the absence of PSII inhibitors (such as 3-(3,4-dichlorophenyl)-1,1-dimethylurea (DCMU)), the IP fluorescence rise may be interpreted as a mixture of photochemical and thermal phase mechanisms. A complete separation of these mechanisms is only possible at saturating light, where both phases contribute in a similar proportion to the total variable Chl *a* fluorescence [4]. However, we will still refer to the IP rise of fluorescence under low light illumination as a thermal phase to illustrate the contribution of the NPQ mechanisms related to the reduction of the PQ pool.

The fast rise of the fluorescence yield from O (F_o) to P (F_m or F_p) is followed within minutes by a fluorescence decrease to a steady-state fluorescence level S or T (F_s), which is close to F_o in healthy leaves. This slow decline of the Chl *a* fluorescence has been shown to be controlled by two major types of quenching mechanisms, i.e. photochemical quenching and NPQ. The photochemical quenching is due to Q_A^- reoxidation, whereas the NPQ results mainly as a consequence of the light-induced formation of a thylakoid pH gradient (i.e. the qE energy-dependent quenching; [11,14]).

Chl *a* fluorescence transients have been linked to PSII heterogeneities on the basis of antenna size, PSII α and PSII β [15,16], the ability to reduce the secondary electron acceptor, Q_B [10], the rate of the PQ reduction [6] and the PQ compartmentation [17,18]. There is evidence that these PSII heterogeneities have consequences on the rate of fluorescence induction. Moreover, Chl *a* fluorescence transients are not only affected by the acceptor side but also by the donor side of PSII. Fluorescence quenching dependent on equilibration on the donor side of PSII (S-states of the oxygen-evolving complex) must also be considered [4,19,20].

Changes in the Chl *a* fluorescence yield are clearly accompanied by variations in the fluorescence lifetime [21,22]. Also, Chl *a* fluorescence emission has been found to be strongly heterogeneous [23–28]. Various models have been proposed to account for the observed fluorescence lifetime heterogeneity (for a review, see Ref. [29]). These models have investigated the lifetimes of PSII fluorescence mostly at the two extreme states of the fluorescence induction (F_o and F_m levels). But so far, no satisfactory correlation between the fluorescence lifetime heterogeneity and the fluorescence induction kinetics has been provided.

The main goal of the present study is to investigate by phase and modulation fluorometry (PMF) the correlation between the kinetic and the temporal heterogeneities of the Chl *a* fluorescence during the whole fluorescence induction in leaves upon a dark-to-light transition. PMF allows simultaneous measurements of both fluorescence lifetime (τ) and yield (Φ) with millisecond sampling rate. We present here experimental evidences leading to the distinction between the different phases of the variable Chl *a* fluorescence on the basis of the pattern of the $\tau-\Phi$ relationship, which exhibits three distinct phases: (i) linear during the OI photochemical phase, (ii) convexly curved during the IP thermal phase, and (iii) linear during the PS phase. Several hypotheses, which could account for the curvature of the $\tau-\Phi$ relationship, are discussed. The curvature of the $\tau-\Phi$ relationship is tentatively explained as a NPQ mechanism related to a transitory conformational change of a pigment–protein complex, probably located on the PSII core antenna.

2. Materials and methods

2.1. Plant material

Various types of green leaves from higher plants were used. However, in this study we present only the results obtained from *Prunus laurocerasus* L., pea (*Pisum sativum* L.), tobacco (*Nicotiana tabacum* L.), wild-type barley (*Hordeum vulgare* L.) and *chlorina* f2 mutant of barley. Mature *P. laurocerasus* leaves were picked from a plant, which was grown outdoors in Orsay (France). Tobacco leaves were grown at the same location in a greenhouse and exposed to full sunlight. Pea, wild- and mutant-type barley plants were grown in a growth chamber at light intensity of 350 μmol photons m^{-2} s^{-1} during a 16/8-h light/dark photoperiod. The temperatures were 24 and 18 °C during the day and night periods, and the relative humidity was 80%. The concentration of Chl per leaf area was estimated by using a SPAD 502 Chl meter (Minolta, Osaka, Japan). Values between 35 and 45 μg/cm^2 of Chl were usually measured, except for *chlorina* f2 where reduced values of 15–20 μg/cm^2 of Chl were observed.

Fluorescence measurements were performed on mature leaves, most of the time still attached to the plant, which were dark-adapted for 1 h in order to ensure a good reproducibility of induction curves. In experiments where the temperature was changed, the sample was placed in a brass holder that was maintained at a constant temperature in the range of 20 to − 20 °C with an accuracy of 0.1 °C. In order to rapidly obtain a low temperature of approximately − 50 °C, a compressed air bomb was used.

2.2. Infiltration of inhibitors

Atrazine and DCMU (CIL Cluzeau, Paris La defense, France) were used to block the electron transfer from Q_A

to Q_B and thus the reoxidation of Q_A^- by PQs. The effect of atrazine and DCMU (10^{-4} M) infiltration on the fluorescence yield and lifetime was studied in barley and pea leaves. In each case, the leaf petiole was cut under water. The leaf was illuminated for 30 min with 100 μmol photons m^{-2} s^{-1} of white light and ventilated, in order to ensure the opening of stomata and transpiration flow prior to the addition of inhibitors. The penetration of the two inhibitors was followed by the decrease of the variable Chl fluorescence using a frequency-induced pulse amplitude modulation (FIPAM) fluorimeter [30]. A complete infiltration of atrazine and DCMU was obtained within 20 min in the case of barley leaves and within 2 h in the case of pea leaves.

2.3. Phase and modulation fluorometry at 54.472 MHz

In this work, a new phase and modulation lifetime fluorometer, with a submillisecond time response, was developed. It is dedicated to kinetic studies of fluorescence lifetimes and yields on photosynthetic systems during the fluorescence induction. The fluorometer was based on a laser-diode excitation at 635 nm (Philips CQL 845, 5 mW; Eindhoven, The Netherlands), which was sinusoidally modulated at 54.472 MHz by a high-frequency signal generator (Hewlett-Packard HP 8656 B; Les Ulis, France). By modulating the injection current of the semiconductor laser, a modulation factor of the laser-diode light better than 98% without distortions was obtained. To avoid thermal drift, the temperature of the laser-diode was maintained constant by a Peltier-based system. The laser light was transmitted through a system of cylindrical lenses to provide uniform intensity across the sample. A variable neutral density filter was used to adjust the laser intensity at the leaf level in the range of 5–700 μmol photons m^{-2} s^{-1}. Fluorescence excitation was initiated by a fast shutter with an opening time better than 400 μs (UniBlitz Electronic VS14; Raleigh, NC). The illuminated area of the sample was approximately 20 mm^2. In order to achieve a higher light intensity of approximately 1500 μmol photons m^{-2} s^{-1}, the laser beam was focused accordingly. The fluorescence was collected by two identical plano-convex Fresnel lenses (f/1, 70 mm diameter) and detected by an avalanche photodiode (Hamamatsu S2384, 3 mm sensitive area diameter, 120 MHz band width; Japan) after passing through a long-pass 665 nm filter (Schott RG 665, 4 mm; Clichy, France). Some measurements were performed using two narrow-band interference filters centered on the two peaks of the Chl fluorescence at 685 nm (Omega, 20 nm full width at half maximum (FWHM)) and 735 nm (Omega, 35 nm FWHM), respectively. The photodetector was part of a resonant circuit with high Q-factor at 54.472 MHz to improve the signal-to-noise ratio. After amplification, a proprietary analog phase-sensitive detector (3 kHz output band width, 0.01° phase sensitivity) analyzed the AC signal. Three parameters were simultaneously acquired corresponding to the fluorescence yield (Φ), the phase (φ) and the demodulation factor (m). The demodulation factor is defined as the ratio of the modulation of fluorescence over the modulation of excitation. These signals were digitized by three multimeters (Hewlett Packard HP 34401A), which set the ultimate sampling rates of the entire system at 700 μs for 512 points or 15 ms for a few thousands points.

As it is well known in the framework of the PMF method, a sinusoidal modulation of the excitation light at a circular frequency ω results in a sinusoidal modulated fluorescence emission at the same frequency as the excitation, but with a reduction in the relative modulation depth and shifted in phase. By measuring the phase (φ) and demodulation factor (m) we can calculate the phase τ_p and modulation τ_m lifetimes of fluorescence [31]:

$$\tau_p = \frac{1}{\omega}\tan(\varphi) \tag{1}$$

$$\tau_m = \frac{1}{\omega}\sqrt{\frac{1}{m^2} - 1} \tag{2}$$

Regardless of the modulation frequency, the phase and modulation lifetimes are equal only in samples characterized by a monoexponential decay. For heterogeneous samples, these lifetimes will differ. In the case of a multi-exponential decay, phase lifetimes are smaller than modulation lifetimes and both decrease with increasing frequency [31]. Although the true lifetimes and relative amounts of each species cannot be determined with single modulation frequency, this provides important qualitative information about the fluorescence heterogeneity of the sample.

Phase delay and modulation ratio of the fluorescence emission were measured relative to a standard of fluorescence. Two different dyes on a solid support were used to calibrate the phase meter. These fluorescence standards, with lifetimes of 0.5 and 2.25 ns to cover the Chl *a* fluorescence lifetimes range in vivo, were previously calibrated with a time-correlated single photon counting (TCSPC) instrument [27]. To minimize the phase drift of the PMF system, the origin of the phase was determined for each fluorescence lifetime measurement. We also determined the dynamic range of the fluorescence intensities, where no corrections for phase and modulation are needed. Moreover, the fluorescence intensity level of the reference was chosen at the middle of the variable fluorescence emitted by leaves. The time resolution estimated from the reproducibility of phase shift measurements was better than a few picoseconds. In the most favorable case, the errors in the determination of apparent lifetimes were estimated to be $\sigma_{\tau p} = 3$ ps and $\sigma_{\tau m} = 8$ ps, corresponding to $\sigma_{\varphi}=0.05^{\circ}$ and $\sigma_{m}=0.0008$, respectively. For a level of fluorescence five times lower, these errors become $\sigma_{\tau p}=10$ ps, $\sigma_{\tau m}=35$ ps, $\sigma_{\varphi}=0.2^{\circ}$ and $\sigma_{m}=0.002$, respectively. The accuracy of measurements can be improved by averaging, given that the noise in phase and modulation is white noise, but this was not necessary in the present work.

2.4. TCSPC lifetime measurements

The fluorescence lifetimes of intact leaves at the F_o level and of the two calibration dyes were determined by a TCSPC instrument previously described [27]. Excitation was provided by a pulsed laser diode at 635 nm with 70 ps pulse duration at 5.4 MHz repetition rate. Fluorescence was imaged after passing through a long-pass filter (Schott RG 665, 4 mm) onto a red sensitive microchannel plate photomultiplier (Hamamatsu R 3809U) by an optical system of two plano-convex lenses. The instrumental response function of the system, estimated from the decay curve of the scattered light, was typically 80 ps (FWHM). A time resolution better than 10 ps was achieved after the deconvolution of the fluorescence decay curve by the Fluomarqt software described elsewhere [32].

2.5. Induction kinetics of fluorescence emission spectra from leaves

Chl fluorescence emission spectra of leaves upon a dark-to-light transition were measured using a computer-controlled spectrofluorometer (Triax 180, ISA Jobin Yvon, Longjumeau, France) with Peltier-cooled charge-coupled device (CCD) detection (16-bit resolution). A laser-diode excitation at 635 nm was used at light intensity of 70 µmol photons m^{-2} s^{-1}. The emitted fluorescence was imaged onto the entrance slit of the spectrograph (*f*/3.9, $f=0.19$ m, 8 nm band pass) by a lens ($f=30$ mm) and an optical fibers bundle. A long-pass 665 nm filter (Schott RG 665, 4 mm) was used to suppress the scattered laser light from fluorescence. The fluorescence spectra were acquired with a sampling rate of 100 ms during the whole fluorescence induction and corrected using an optical radiation calibrator (LI-COR 1800-02, Lincoln, NE, USA).

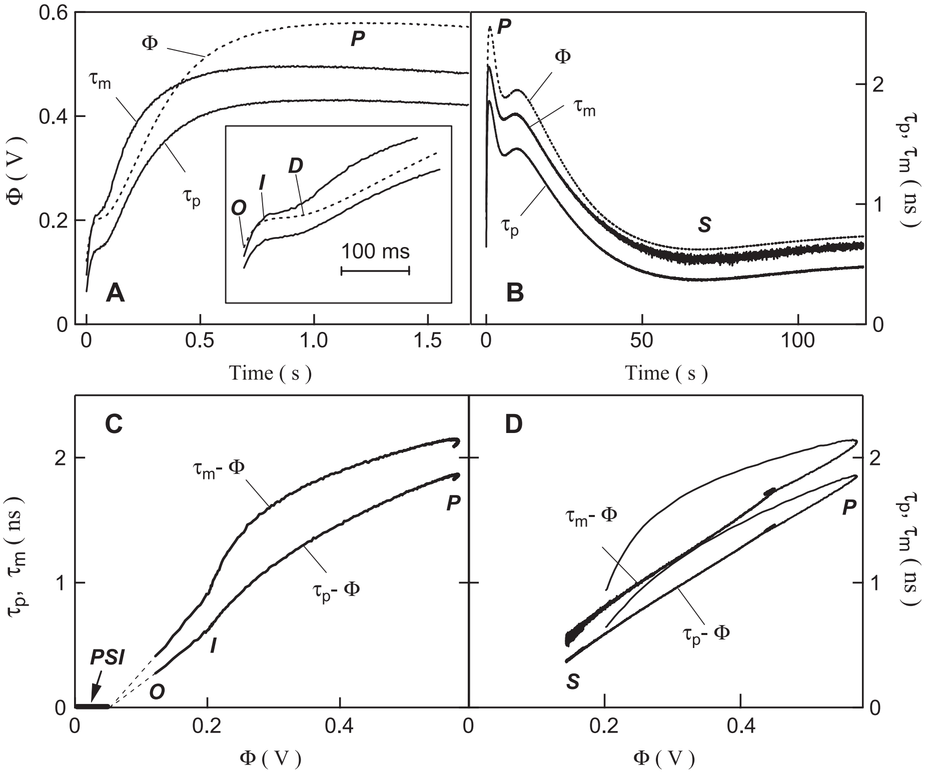

Fig. 1. Typical induction curves of fluorescence yield (Φ) and phase and modulation lifetimes (τ_p and τ_m) obtained with the PMF system at 54.472 MHz in a dark-adapted pea leaf. The actinic light intensity was 100 µmol photons m^{-2} s^{-1}. The fluorescence was detected through a wide-band RG 665 filter. Two time scales, 1.6 s (3 ms sampling rate) and 120 s (15 ms sampling rate), respectively, were used to investigate: (A) the OIP fast rise phase; (B) the PS slow decay phase. In (A), the inset shows a zoom of the beginning of the fluorescence induction (Φ—dashed curve, τ_p and τ_m—solid curves with $\tau_m > \tau_p$). The $\tau-\Phi$ relationships during the experiments (A) and (B) are shown in (C) and (D), respectively. The $\tau-\Phi$ relationship varied corresponding to three distinct phases: (i) linear during the OI photochemical phase, (ii) convexly curved during the IP thermal phase, and (iii) linear during the PS phase. Extrapolation of the $\tau-\Phi$ relationship during the OI phase gives the contribution of PSI.

3. Results

3.1. $\tau - \Phi$ Relationship during the fluorescence induction in dark-adapted leaves

The induction kinetics of fluorescence yield (Φ), phase (τ_p) and modulation (τ_m) lifetimes of a dark-adapted pea leaf at two time scales are shown in Fig. 1A and B. The intensity of the actinic light was 100 μmol photons m^{-2} s^{-1}, leading to a F_v/F_p ratio of approximately 0.785. The $\tau - \Phi$ relationship for both τ_p and τ_m exhibits a typical pattern that is related to the different phases of the fluorescence induction (Fig. 1C and D). During the fast OI photochemical phase, both Φ and τ increase in parallel due to progressive Q_A reduction, and the $\tau - \Phi$ relationship is linear (Fig. 1C). A positive abscissa intercept of the linear $\tau - \Phi$ relationship was systematically obtained (Fig. 1C), except for *chlorina* f2 leaves where extrapolation of the line was very close to the origin (data not shown, see Discussion). During the IP thermal phase, dominated by the reduction of the PQ pool, this relationship displays a pronounced convex (upward) curvature (Fig. 1C and D). Further, the slow decrease of the fluorescence from P to S again shows proportionality between yield and lifetime (Fig. 1B). Therefore, an almost linear $\tau - \Phi$ relationship is observed (Fig. 1D). Considering their distinct characteristics, the OI, IP and PS phases constitute an intrinsic heterogeneity of the variable Chl *a* fluorescence, which is not related either to the PSII antenna or PSII reducing side heterogeneities. This pattern was found in all of the control plants we examined in this study and it seems to be universal for all plant species.

A value of τ_p smaller than τ_m measured during the entire fluorescence induction is the indication of a heterogeneous emission, generated by the superposition of several components with different lifetimes. The difference between τ_p and τ_m was approximately 200–300 ps at the peak of fluorescence in all control leaves and was almost constant during the slow PS decline, since induction curves of the τ_p and τ_m lifetimes were parallel (Fig. 1B and D). However, we noted that the convex curvature of the $\tau - \Phi$ relationship during the IP phase was always more pronounced for τ_m than for τ_p. In the framework of the PMF method, this suggests that a long lifetime fluorescence component is involved (see companion paper: N. Moise and I. Moya, Correlation between lifetime heterogeneity and kinetics heterogeneity during chlorophyll fluorescence induction in leaves: 2. Multi-frequency phase and modulation analysis evidences a loosely connected PSII pigment–protein complex). It can be also seen in Fig. 1A that the peak (P) of the fluorescence yield curve is clearly delayed compared to the peak of fluorescence lifetime inductions, and that the induction curves of fluorescence yield and lifetimes have different rise kinetics, which account for the curvature of the $\tau - \Phi$ relationship.

To verify that no changes in absorption occurred during the fluorescence induction that could produce the curvature of the $\tau - \Phi$ relationship, we measured, in addition to fluorescence, the reflected and the transmitted laser radiation at 635 nm. It is important to note that no absorption changes were found (data not shown).

We also checked that the first point of the fluorescence induction measured with our PMF instrument was close to the real F_o. To do this, we measured the Chl *a* fluorescence decay on different leaves at the F_o level with the TCSPC system. We used the lifetime and yield values accounting for the fluorescence heterogeneity at F_o to calculate the τ_p and τ_m lifetimes corresponding at 54.472 MHz and we found them to agree well with those measured directly by PMF (data not shown; for similar results, see Ref. [33]).

3.2. Atrazine and DCMU effect

We investigated the effect of atrazine and DCMU, known to block the electron transfer from Q_A^- to PQs [11,34], on the fluorescence induction curves and $\tau - \Phi$ relationship. The inset of Fig. 2 shows the induction curves of fluorescence yield and lifetimes obtained under low actinic light (70 μmol photons m^{-2} s^{-1}) on a dark-adapted pea leaf infiltrated with atrazine. We note that in the presence of this inhibitor, the fluorescence rise time is decreased, but the $\tau - \Phi$ relationship still displays a convex curvature (Fig. 2), although less pronounced than in the absence of inhibitor. This result was also obtained in the case of infiltrated barley (wild-type and *chlorina* f2) leaves with atrazine and DCMU (data not shown). The IP thermal phase was completely suppressed, whereas the amplitude of the OI photochemical phase was increased [4,9,35]. Therefore, the fluorescence induction in the presence of these PSII inhibitors will reflect the

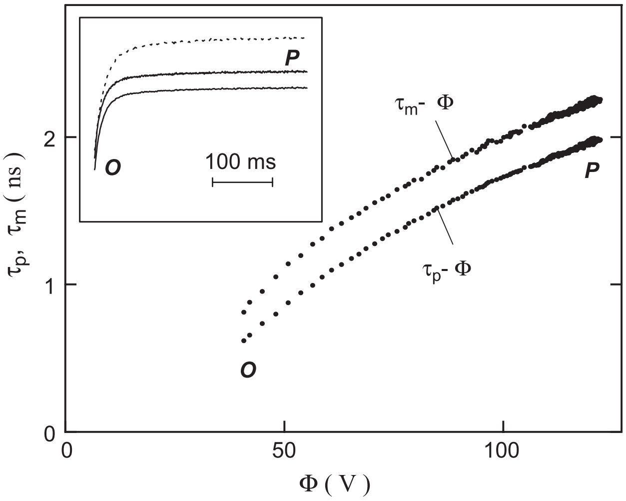

Fig. 2. $\tau - \Phi$ Relationships during the OP rise phase of the fluorescence induction in atrazine (10^{-4} M) infiltrated pea leaf. The light intensity was 70 μmol photons m^{-2} s^{-1}. The inset shows the induction curves of the fluorescence yield Φ (dashed curve) and the lifetimes τ_p and τ_m (solid curves with $\tau_m > \tau_p$) measured with 700 μs sampling rate.

Table 1
Effect of atrazine and DCMU infiltration (10^{-4} M) on the fluorescence yield (Φ) and lifetimes (τ_p, τ_m) measured with PMF (54.472 MHz) at the F_m level

	Wild barley			*Chlorina* f2		
	Φ (a.u.)	τ_p (ns)	τ_m (ns)	Φ (a.u.)	τ_p (ns)	τ_m (ns)
Control	760	2.2	2.3	390	1.7	2.0
Atrazine	24%	11.3%	10.9%	12.8%	11.7%	12.5%
Control	720	2.18	2.29	370	1.72	2.05
DCMU	22%	16%	17%	25%	18%	19%

Control and inhibitor infiltrated leaves of wild-type barley and *chlorina* f2 mutant were measured with 1500 µmol photons m^{-2} s^{-1} light. Percentages represent the decrease after the addition of the inhibitor.

photochemical reduction of Q_A only. However, a fluorescence NPQ related to the oxidized PQ pool still exists [13].

3.3. Quenching by oxidized PQ pool

To investigate the nature of the quenching induced by oxidized PQs, we compared the fluorescence induction curves of control leaves with those of atrazine and DCMU-infiltrated leaves. Wild-type and *chlorina* f2 barley leaves were used for this study. The fluorescence yield and lifetime induction curves were measured by PMF under high light intensity (1500 µmol photons m^{-2} s^{-1}), so that the F_m level in control leaves was obtained. The fluorescence emission was analyzed with a narrow interference filter centered at 685 nm (20 nm FWHM) to reduce the fluorescence heterogeneity. We found a significantly smaller fluorescence yield (Φ) at the maximum fluorescence level in infiltrated leaves (oxidized PQs state), as compared with control leaves (reduced PQs state). More importantly, the lifetimes τ_p and τ_m were also decreased by the quenching process. The extent of this quenching, attributed to the oxidized PQ pool, was found to be 10–25% (Table 1) in agreement with many previous studies. We note that the quenching was larger in the case of DCMU than atrazine infiltration.

3.4. Low-temperature effect

Decreasing the temperature of leaves resulted in significant changes in the fluorescence induction curves and $\tau-\Phi$ relationship; indeed, temperature is known to play an important role in thermal phase mechanisms [4,11]. By decreasing the temperature to approximately −20 °C the OI phase increased without a major modification of the total variable fluorescence. Both the OI photochemical and the IP thermal rise phases were slowed down and the relative proportion of each phase was altered. The inset of Fig. 3A shows the induction curves of fluorescence yield and lifetime under low actinic light (70 µmol photons m^{-2} s^{-1}) for a tobacco leaf at −10 °C. In this experiment, only the phase lifetime τ_p was measured. It is worth noting that an almost linear $\tau-\Phi$ relationship during both the IP thermal and OI photochemical phases was obtained (Fig. 3A).

Below −50 °C the thermal phase is completely suppressed, leading to an apparently monophasic rise of fluorescence yield and lifetimes (Fig. 3B, inset). Neubauer and Schreiber [4] have reported a similar behavior for the fluorescence yield induction at low temperature down to −70 °C in spinach leaves and saturating light intensities. Like the fluorescence induction at room temperature in the presence of atrazine, the fluorescence rise at low temperatures reflects only the photochemical reduction of Q_A [11]. However, at low temperature the $\tau-\Phi$ relationship was found to be linear (Fig. 3B). A further analysis revealed that the $\tau-\Phi$ relationship was still biphasic with two slightly different slopes. Compared with room temperature, a pronounced decrease in the maximal fluorescence values for both yield and lifetimes was observed. This is a clear evidence for the presence of NPQ due to oxidized PQ pool (see Discussion).

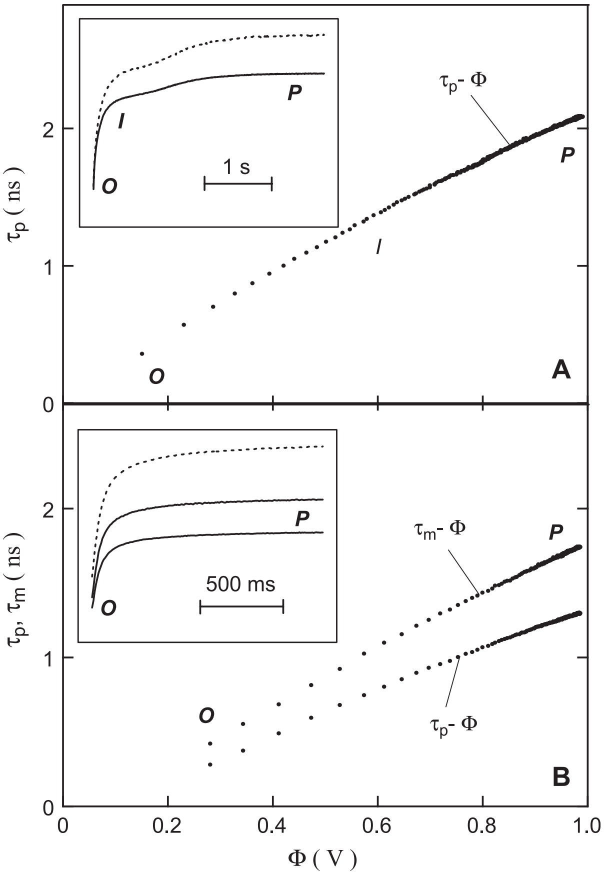

Fig. 3. $\tau-\Phi$ Relationships during the OIP rise phase of the fluorescence induction at low temperature: (A) −10 °C in dark-adapted tobacco leaf. The light intensity was 70 µmol photons m^{-2} s^{-1}. The inset shows the induction curves of the yield Φ (dashed curve) and the lifetime τ_p (solid curve) measured with 3 ms sampling rate. (B) −50 °C in dark-adapted pea leaf. The light intensity was 100 µmol photons m^{-2} s^{-1}. The inset shows the induction curves of the yield Φ (dashed curve) and the lifetimes τ_p and τ_m (solid curves with $\tau_m > \tau_p$) measured with 3 ms sampling rate.

3.5. Spectral dependence of the $\tau-\Phi$ relationship

The heterogeneity of the Chl *a* fluorescence is partly due to the existence of two photosystems (PSI and PSII) which have different contributions in the red and far-red regions of the spectrum. At room temperature, most of the fluorescence at 685 and 735 nm arises from PSII [2,11] with minor contribution of PSI fluorescence at 730 nm [11,36]. Compared to dilute chloroplast suspensions, the fluorescence spectra and kinetics from leaves are more complicated due to their optical properties (high optical density, strong scattering of incident light and differential reabsorption of fluorescence). Thus, in order to analyze more carefully the $\tau-\Phi$ relationship, the fluorescence was detected in a narrow spectral band using two interference filters centered at 685 nm (20 nm FWHM) and 735 nm (35 nm FWHM), respectively (Fig. 4). Measurements were performed under the same conditions as for Fig. 1, on the same spot on the leaf, after a dark-time interval allowing a good reproducibility of the induction curves. For these two spectral bands, the F_v/F_p ratio was 0.815 and 0.755, respectively. The signal-to-noise ratio was slightly larger at 735 than at 685 nm as a result of higher fluorescence intensity.

We noted that the $\tau-\Phi$ relationships for red and far-red fluorescence (Fig. 4) look similar to the ones recorded under wide-band detection (Fig. 1), that is the $\tau-\Phi$ relationship pattern is qualitatively independent of the fluorescence analyzing wavelength. However, when the fluorescence is measured in a narrow band about 685 nm, only PSII fluorescence is detected. In this case, the linear OI phase extrapolates to zero (Fig. 4A). We thus concluded that the positive yield-axis intercept of the $\tau-\Phi$ relationship obtained in PMF experiments is due to contribution of the constant PSI fluorescence (see also Refs. [33,37]). In leaves, the high reabsorption of the fluorescence at 685 nm tends to enhance the PSI contribution [38–41]. Moreover, the avalanche photodiode detector used in our instrument, which has an enhanced sensitivity in the infrared region, amplified the contribution of the far-red fluorescence emission.

The τ_p and τ_m lifetimes measured at 685 nm were larger than those measured with the wide-band RG 665 filter, whereas the τ_p and τ_m lifetimes measured at 735 nm were smaller. Also, the difference between τ_p and τ_m at 685 nm decreased to only 100 ps (Fig. 4A and B), whereas this difference increased to 330–350 ps when measured at 735 nm (Fig. 4C and D). These findings are a consequence of changes in the fluorescence heterogeneity. Indeed, by using the 685 nm filter, the PSI short lifetime contribution was removed and the fluorescence heterogeneity was diminished, leading to greater τ_p and τ_m lifetimes and closer to each other. The use of the 735 nm filter had the opposite effect due to enhanced contribution of the PSI short

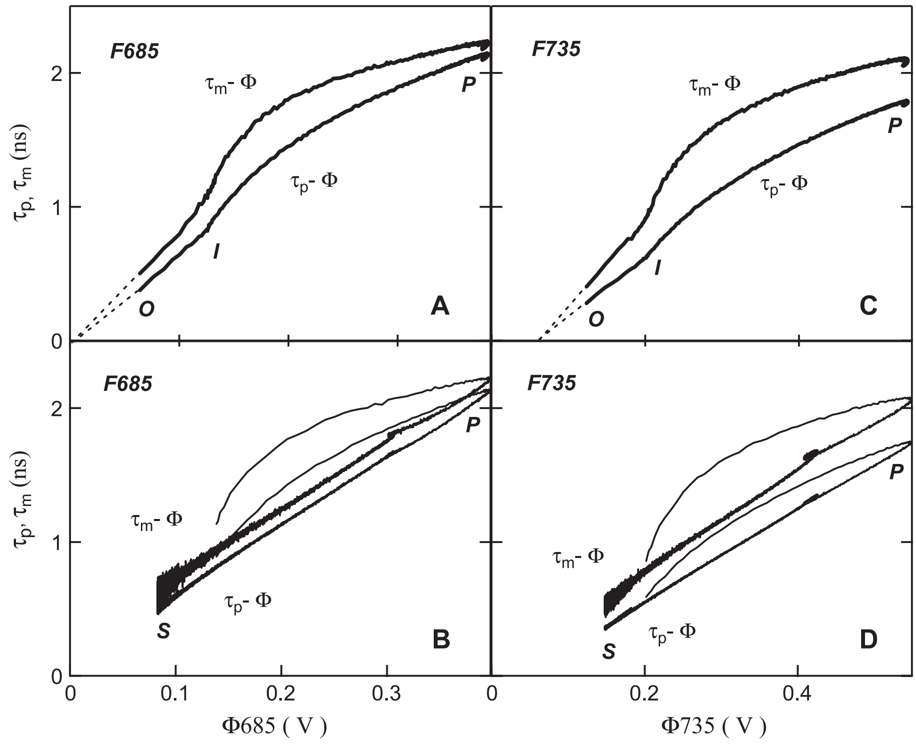

Fig. 4. $\tau-\Phi$ Relationships of the fluorescence induction in dark-adapted pea leaves detected with two narrow-band interference filters centered at 685 nm (20 nm FWHM) and 735 nm (35 nm FWHM), respectively. For each detection filter, two time scales were used for the fluorescence induction, 1.6 s (A and C) and 120 s (B and D). Measurements taken under the same experimental conditions as for Fig. 1.

lifetime to the measured fluorescence. Only in *chlorina* f2 mutant leaves, did changing the detection filter not affect the values of τ_p and τ_m lifetimes (data not shown, see Discussion).

3.6. Φ685 versus Φ735 relationship

Measurements of the fluorescence induction yields at the 685 and 735 nm bands allowed us to investigate the correlation between the fluorescence emitted at the two peaks of the Chl *a* fluorescence spectrum. Fig. 5 shows the $\Phi685-\Phi735$ relationship on two time scales. It is worth noting that this plot appears similar to the $\tau-\Phi$ relationship. A similar $\Phi685-\Phi735$ relationship has been previously observed upon simultaneous measurements of the fluorescence induction curves at $\lambda < 690$ nm versus $\lambda > 715$ nm [42–44]. It is thus very likely that the curvature of the $\tau-\Phi$ and $\Phi685-\Phi735$ relationships during the IP phase has the same origin (see Discussion).

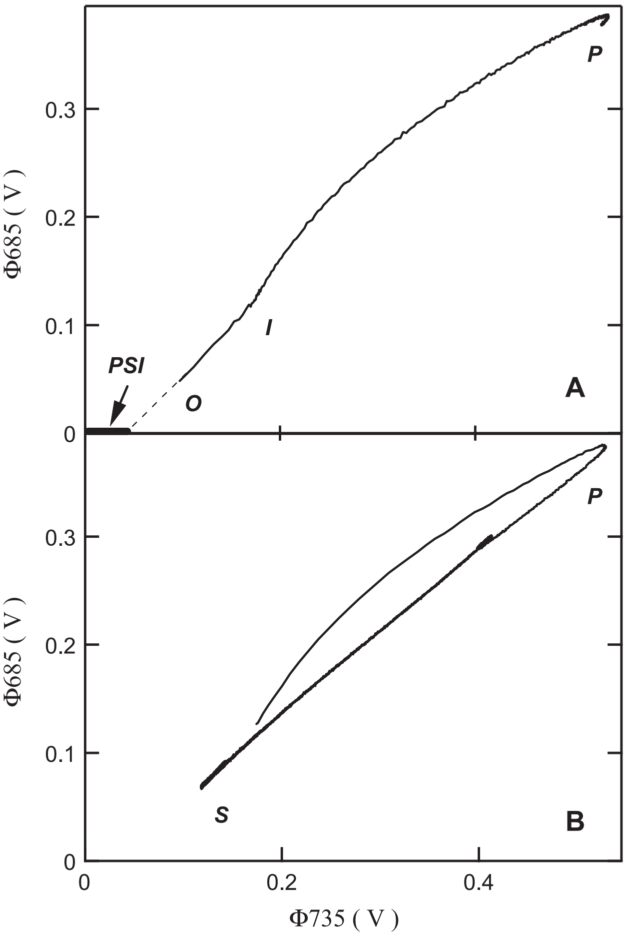

Fig. 5. $\Phi685-\Phi735$ Relationship of the fluorescence induction in a dark-adapted pea leaf on two different time scales: (A) OIP phase; (B) PS phase. Results obtained from Fig. 4. $\Phi685-\Phi735$ Relationship is similar with the $\tau-\Phi$ relationship. Extrapolation of the linear $\Phi685-\Phi735$ relationship during the OI phase gives the contribution of PSI.

4. Discussion

In the past, the $\tau-\Phi$ relationship has been analyzed exclusively in the framework of a model of energy circulation among PSII units. In this work, we discuss the pattern of the $\tau-\Phi$ relationship, particularly the deviation from linearity, from a more detailed perspective. To explain the observed convex curvature during the thermal phase, we tested several hypotheses, commonly associated with the fluorescence induction: PSII units connectivity, quenching by the oxidized PQs, variable spillover, reabsorption effects. None of these hypotheses could explain our data. Thus, we are lead to introduce a new hypothesis as a conformational change of a PSII pigment–protein complex.

4.1. PSII units connectivity and τ–Φ relationship

Various models have been considered for the antenna organization in the photosynthetic membrane [29,45]. Each model predicts a different behavior of the $\tau-\Phi$ relationship. In the "separate units model", where no energy transfer between PSII units can occur, the fluorescence decay profile is expected to be biexponential and the mean $\tau-\Phi$ relationship to be convex, or more precisely, a branch of an equilateral hyperbola [21]. The fluorescence decay will consist of a mixture of two constant lifetimes: a short lifetime for open reaction center units and a long lifetime for closed reaction center units. Only their amplitudes change, depending on the proportion of closed reaction centers, whereas the lifetimes are constant during the whole fluorescence induction.

In the "lake model", the PSII units have only a statistical significance and the PSII reaction centers are embedded in a "lake" of connected pigments. This model predicts monoexponential fluorescence decay, which changes continuously when PSII reaction centers are progressively closed, and a linear relationship between τ and Φ following the scheme of a dynamic quenching [21].

In an intermediate case, the "connected units model", there is some connectivity among PSII units with some restriction to free excitation energy circulation [29,45]. Depending on the number of reaction centers that are connected, the probability of energy transfer between PSII units, and the degree of PSII trap closure, fluorescence lifetimes can range between the F_o and F_m lifetimes. Different fluorescence components exhibit complex variations in both amplitude and lifetime leading to a $\tau-\Phi$ relationship intermediate between the limiting cases.

Experimentally, the earliest phase fluorometry measurements showed a linear $\tau-\Phi$ relationship, which was interpreted as supporting the lake model [46,47]. However, deviations from the abovementioned linearity have also been reported [21,22]. The convex $\tau-\Phi$ relationship measured in this case was analyzed in the framework of a model of connected units with a certain degree of energy exchange [21]. Furthermore, an earlier investigation of the $\tau-\Phi$

dependence in leaves of higher plants concluded that at least two lifetime components were required to account for the convex curvature of the $\tau-\Phi$ relationship and that the lake model was therefore questionable [22].

TCSPC measurements have shown that the progressive closure of PSII reaction centers by light, in the presence or absence of PSII inhibitors, induces continuous changes in the lifetime and yield of each PSII fluorescence component [24,25,48–50]. Therefore, these results are clearly inconsistent with the hypothesis of the model of separate units and suggests instead a high degree of connectivity between PSII units in leaves.

4.2. Optical and spectral effects

Compared to dilute chloroplasts suspensions, intact leaves have a complex structure, with a high optical density, and induce a strong scattering of the incident light. The excitation light is attenuated when penetrating the leaf, inducing intensity gradients in its whole depth [51]. As a result, the fluorescence induction kinetics generated at different depths in the leaf will have different rise-times and amplitudes. On the other hand, depending on the wavelength, the emitted Chl *a* fluorescence will be differentially reabsorbed by the photosynthetic pigments. The fluorescence will be reabsorbed to a greater extent at 685 nm than at wavelengths beyond 700 nm. Consequently, the fluorescence emitted at 685 nm will come from a thin layer at the surface of the leaf, whereas deeper layers will contribute more to the fluorescence signal measured at non-reabsorbed wavelengths. Regarding this point, based on simulations of the integrated Beer–Lambert's law, it was established that the time course of the fluorescence induction measured at 735 nm is slower than the one measured at 685 nm [52]. Our simulations also showed that an incurvation of the $\tau-\Phi$ relationship could be generated by different time courses of the fluorescence induction within the leaf (data not shown).

However, our results clearly show that the optical effects are not responsible for the curvature of the $\tau-\Phi$ relationship. Although the fluorescence heterogeneity was reduced when using two narrow-band interference filters centered at the fluorescence peaks, we found that the $\tau-\Phi$ relationships of the variable fluorescence at 685 and 735 nm bands on a normalized scale are identical, exhibiting the same curvature (data from Fig. 4). If the non-linearity of the $\tau-\Phi$ relationship was solely due to reabsorption effects, we would expect the $\tau-\Phi$ relationship at 685 nm to be more linear than at 735 nm. Indeed, Malkin et al. [22] showed that if the original relation between τ and Φ is linear for the fluorescence contribution from each cross-section along the actinic light path in the leaf, the integrated $\tau-\Phi$ relationship measured at 685 nm still remains linear within 1% error. Therefore, we conclude that the non-linearity of the $\tau-\Phi$ relationship at the two wavelengths has the same physical origin, and it does not depend on the spectral differences.

Other results are in line with our conclusion. PMF measurements performed in a 2 mm optical path length cell on diluted chloroplasts and algae suspensions with Chl concentrations between 2 and 10 μg/ml have shown the same striking $\tau-\Phi$ relationship pattern (Goulas, Y. and Moya, I., unpublished data). Moreover, the curvature of the $\tau-\Phi$ relationship during the IP phase was comparable with that presented in our results for leaves.

Butler and Strasser [53] have studied the reabsorption effects in chloroplast suspensions at high Chl concentrations up to 40 μg/cm^2 and at low temperatures (− 196 °C). Despite the fact that reabsorption strongly affects the emission spectrum, they concluded that neither the F_v/F_o ratio nor the value of direct absorption by PSI were affected. More importantly, irrespective of the chloroplast concentration, they found a linear relationship between the fluorescence measured at 694 and 730 nm during the fluorescence induction, in contrast with the curved relationship that we observed at room temperature. This result is consistent with our observation that the $\tau-\Phi$ relationship during the IP phase of the fluorescence induction in leaves becomes linear at low temperature (Fig. 3). Since the Chl content is the same, reabsorption effects should not be significantly changed.

Reabsorption effects on Chl fluorescence decays were also discussed by Terjung [54], who concluded that, even in leaves, the Chl *a* fluorescence lifetime measurements do not require corrections due to the high pigment content.

4.3. Variable “spillover” hypothesis

Our PMF measurements show that the relationship between the fluorescence yield at 685 and 735 nm (Fig. 5) is similar to the $\tau-\Phi$ relationship (Fig. 4). It is very likely from this similarity that the curvature of the $\tau-\Phi$ and $\Phi685-\Phi735$ relationships has a common origin. A similar $\Phi685-\Phi735$ relationship in leaves was previously reported [42–44]. Rapid energy distribution changes between PSII and PSI (variable spillover) have been proposed to account for the non-linearity in the $\Phi685-\Phi735$ relationship [42,43]. However, it is worth noting that in the framework of connectivity between PSII units, either total or partial, any first-order de-excitation mechanism that acts at the antenna level or the PSII reaction center should produce dynamic variations in the fluorescence properties and would therefore maintain a linear $\tau-\Phi$ relationship. This is the case for spillover, as far as the excitation energy transfer from PSII to PSI can be described as a first-order de-excitation pathway of the PSII antenna excited pigments [29,55].

Two further experimental arguments can be invoked here to disprove that the $\tau-\Phi$ curvature could be due to spillover. First, fluorescence induction kinetics obtained by PMF in PSII isolated particles (BBY) showed a similar curvature of the $\tau-\Phi$ relationship during the IP phase (Goulas, Y. and Moya, I., unpublished data). We note that in this material, no spillover can occur due to the lack of PSI. Second, it is known that *chlorina* f2 barley mutant grown in low light has a reduced level of PSI antenna [56]. Therefore, we expected that spillover is reduced in *chlorina* f2 compared with wild-type barley leaves. Nevertheless, the PMF measurements showed that wild-type and *chlorina* f2 barley leaves exhibit the same curvature of the $\tau-\Phi$ relationship. An independent confirmation of the lack of PSI antenna in our *chlorina* f2 barley leaves comes from the fact that the $\tau-\Phi$ relationship of the linear OI phase extrapolates to zero and from the lack of changes in fluorescence lifetimes with the fluorescence analyzing filter, 685 versus 735 nm (data not shown).

4.4. Quenching by the oxidized PQ pool

A substantial quenching of the F_m fluorescence level (10–30%) has been found in isolated thylakoids in the presence of DCMU and has been attributed to the oxidized PQ pool [13,57,58]. There is clear evidence that this quenching is nonphotochemical in nature and that it is not due to an inhibition on the donor side of PSII by DCMU [59]. Kramer et al. [60] found a significant reduction in F_v/F_o (25–38%) in atrazine-infiltrated leaves of different plants. They also attributed this NPQ to the oxidized PQ pool.

The kinetics of the IP thermal phase is known to reflect the reduction of the PQ pool [1,9,11,12]. We therefore investigated whether the $\tau-\Phi$ relationship curvature measured during the IP phase of the fluorescence induction was related to the quenching by oxidized PQ molecules. Accordingly, we studied the effect of atrazine and DCMU infiltration on the maximal fluorescence yield and lifetimes of wild-type and *chlorina* f2 barley leaves. Importantly, we found that the presence of these inhibitors decreases not only the fluorescence yield but also the lifetimes. This quenching could be clearly assigned to the oxidized PQ pool. Its extent is between 10% and 25% (Table 1), in agreement with previous studies. The existence of this quenching was also observed in the case of *chlorina* f2 suggesting that the quenching by oxidized PQs occurs at the level of the PSII antenna core complexes rather than at the light-harvesting complex of PSII (LHCII) (see below).

Earlier fluorescence lifetime and yield measurements agree with our results. Moya [61] found by PMF that the addition of DCMU to FL5 *Chlamydomonas* mutants lacking PSI reaction centers [62] decreased both the fluorescence yield and mean lifetime at the F_m level by 10%. Using the method of saturating pulses and TCSPC detection, a significant decrease of the mean fluorescence lifetime (10%, from 2.0 to 1.8 ns) was found when DCMU was infiltrated in wild-type barley leaves [63,64].

Finally, from PMF measurements at low temperature (− 50 °C) we obtained a significant quenching of the maximal fluorescence level, both in lifetimes and yield (Fig. 3B). We again assign this quenching to oxidized PQs since the PQ pool remains fully oxidized during the dark-to-light transition at low temperature [11].

These results allow us to conclude that the mechanism of the quenching by oxidized PQs is essentially dynamic as it affects both fluorescence yield and lifetimes [65]. If this were a static mechanism, as was recently proposed by Kurreck et al. [66], quenching by the oxidized PQ pool would leave the fluorescence lifetime unchanged. On the basis of its dynamic nature, it appears clear that this quenching cannot explain the convex curvature of the $\tau-\Phi$ relationship.

In view of this conclusion, we can further discuss the influence of the PQ pool heterogeneities on the $\tau-\Phi$ relationship. These heterogeneities are due to compartmentation of PQs within domains characterized by different PQ/center stoichiometry and different photoreduction time [17,67,68]. Although this is an important factor that affects the fluorescence rise kinetics, we stress that the $\tau-\Phi$ relationship does not depend on PQ heterogeneity, neither spatially nor kinetically, because the quenching by oxidized PQs is dynamic. Therefore, the photoreduction of different pools of PQs will affect in parallel the fluorescence yield and the fluorescence lifetime leading to a linear $\tau-\Phi$ relationship.

4.5. The fast conformational changes hypothesis

The possible origins of the fluorescence induction thermal phase have been discussed in a recent review [7] but none of the known hypotheses can explain our data. Bradbury and Baker [69] resolved a significant and variable NPQ accompanying variable photochemical quenching during rapid induction of fluorescence from O to P in dark-adapted pea leaves and isolated thylakoids. They also found that this quenching is still present in DCMU-infiltrated leaves and thylakoids during the fast rise of the fluorescence induction. They concluded that the light-induced charge separation across the thylakoid membrane might be the origin of this NPQ.

We interpret our results in the framework of a variable and transitory NPQ that is responsible for the curvature of the $\tau-\Phi$ relationship during the IP phase. This quenching was not removed by atrazine and DCMU infiltration, in agreement with the results of Bradbury and Baker [69]. In the presence of these inhibitors, the $\tau-\Phi$ relationship remains non-linear (Fig. 2). We also note that similar results were obtained in wild-type barley and Chl *b*-deficient *chlorina* f2 mutant of barley. In *chlorina* f2, many of the complexes of LHCII (Lhcb1, Lhcb2, Lhcb3) and minor antenna (Lhcb4, Lhcb5, Lhcb6 also known as CP29, CP26, CP24, respectively) are absent or highly reduced [70–75]. Moreover, in the absence of the Chl *b*, these proteins (Lhcb1-6) cannot form stable pigment–protein complexes neither in vitro nor in vivo (R. Bassi, personal communication). Therefore, our data suggest that the quenching responsible for the curvature of the $\tau-\Phi$ relationship it is very likely to occur at the level of the PSII core antenna complexes. Further arguments favoring this hypothesis are presented in the companion paper.

Furthermore, based on the similarity between the $\tau - \Phi$ and $\Phi 685 - \Phi 735$ relationships, we propose the hypothesis that a conformational change in one pigment–protein complex of the PSII core antenna takes place during the IP thermal phase of fluorescence induction. This conformational transformation accounts for the variable NPQ and is thus responsible for the curvature of $\tau - \Phi$ relationship. Indeed, it has already been observed that conformational changes of photosynthetic pigments could drastically affect both the fluorescence yield and lifetime [76,77] and the correlation between these parameters is not linear [78,79]. Moreover, conformational changes of proteins can occur without any accompanying change in the absorption spectra [80], as it happens in our work.

Conformational changes affecting a pigment–protein complex are likely to be accompanied by changes of the fluorescence spectra [81]. To test whether such spectral changes take place, we measured the fluorescence spectra of leaves during the whole fluorescence induction. Fig. 6 shows the induction of Chl fluorescence spectra in a *P. laurocerasus* leaf upon a dark-to-light transition. A detailed analysis of these spectra revealed that the red peak at 685 nm shows a transitory and variable blue shift during the IP thermal phase, whereas the position of the far-red peak at 735 nm remains unchanged. This variable shift has a maximum amplitude of approximately 1 nm at the middle of the induction curve and clearly appears to be associated with the curvature of both $\tau - \Phi$ and $\Phi 685 - \Phi 735$ relationship. Contrary to the fast fluorescence rise, the position of both peaks remains constant during the slow fluorescence decline. Consequently, linear $\tau - \Phi$ and $\Phi 685 - \Phi 735$ relationships were obtained. The spectral change is a striking result, which has not been observed previously, and clearly supports the hypothesis that a conformational change is involved during the IP phase of the fluorescence induction.

Independent evidence for conformational change hypothesis was obtained from the PMF measurements in leaves at subfreezing temperatures. The main effect of the low temperature is the linearization of the $\tau - \Phi$ relationship during the IP phase (Fig. 3A). To explain this result one may assume that at subfreezing temperatures conformational changes in thylakoid membranes are inhibited.

The conformational change established in this work differs in several respects from the conformational change already observed both in vitro and in vivo in the pigment–protein complexes of LHCII [76,81,82]. This phenomenon has been related to the LHCII aggregation as a mechanism of NPQ [83–85]. First, the conformational change invoked here acts in the first second of illumination during the fast IP phase, whereas the LHCII aggregation starts during the slow PS decline phase, thus requiring minutes of exposure to light. Second, the conformational change observed during the IP phase results in a blue shift of the Chl *a* fluorescence spectra and does not induce changes in the absorption, whereas a red shift of the fluorescence emission spectrum accompanied by a red shift in the Chl absorption maximum was observed for the aggregation of LHCII [76,78,86].

After the fluorescence induction reaches its peak, the conformational changes are no longer observed, as indicated by the constant position of the red peak of the fluorescence spectra during the PS phase. The decrease of the fluorescence yield is due to the Q_A^- reoxidation and to the

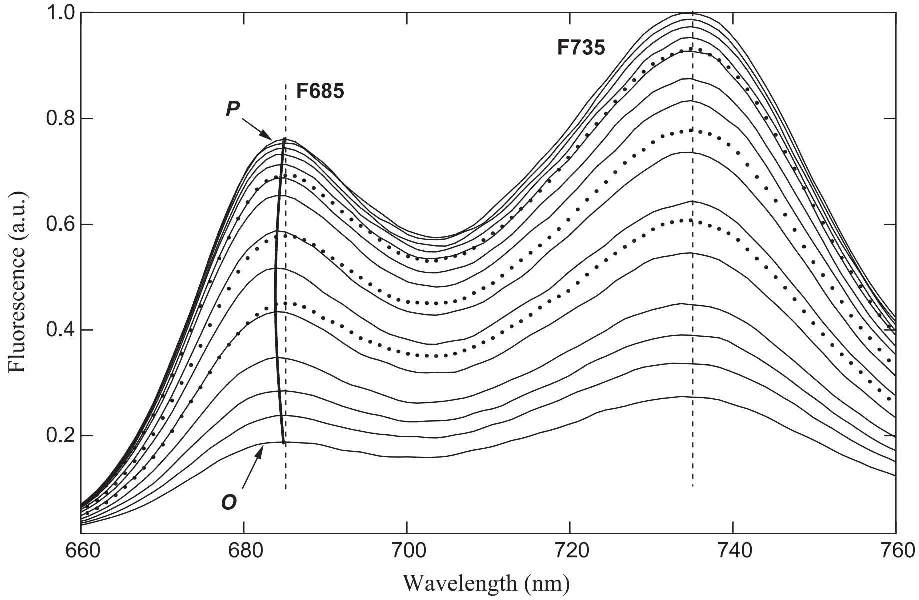

Fig. 6. Induction of the Chl *a* fluorescence spectra upon a dark-to-light transition in a *P. laurocerasus* leaf at light intensity of 70 μmol photons m^{-2} s^{-1}. The fluorescence spectra were recorded with 100 ms sampling rate during the fluorescence transient (solid curve for the OIP phase and dotted curve for the PS phase). The curved line shows the transient blue shift of the 685 nm peak during the IP phase. Its maximal amplitude is about 1 nm. The dotted lines show the position of the red and far-red peaks at F_o, F_p and some intermediary fluorescence levels during the PS phase. The position of the 735 nm peak was unchanged during the whole fluorescence induction.

development of the energy-dependent quenching (qE). This quenching exhibits a dynamic behavior for the different components of the PSII Chl *a* fluorescence emission [63,64] similarly affecting the fluorescence quantum yield and lifetime. Thus, this explains that the $\tau-\Phi$ relationship is linear during the PS phase (see also the companion paper).

The present work shows that a variable and transitory NPQ is responsible for the curvature of the $\tau-\Phi$ relationship during the IP thermal phase of the fluorescence induction. We propose to interpret it as a conformational change of a pigment–protein complex located on the PSII core antenna but its nature is still unclear. The question of the nature of photophysical process responsible for conformational change and its physiological role remains open. The companion paper describes a decomposition of the fluorescence lifetime heterogeneity during the whole fluorescence induction and provides some additional information on this phenomenon.

Acknowledgements

We thank Dr. Z.G. Cerovic, Dr. J. Lavergne, Dr. J.-M. Ducruet, Dr. F. Morales, Dr. J. Cavender-Bares, Dr. G. Parlant and Dr. D. Parent for stimulating discussions and useful suggestions on the manuscript. Thanks are also due to Dr. Y. Goulas and Dr. M. Bergher for helpful discussions. This work was supported by CNRS through the GDR #1536. N. Moise gratefully acknowledges the "Réseau Formation-Recherche Franco-Roumain" #97P4701, the LURE and the CNRS for their financial support.

References

[1] H. Dau, Short-term adaptation of plants to changing light intensities and its relation to photosystem II photochemistry and fluorescence emission, J. Photochem. Photobiol., B Biol. 26 (1994) 3–27.

[2] Govindjee, Sixty-three years since Kautsky: chlorophyll *a* fluorescence, Aust. J. Plant Physiol. 22 (1995) 131–160.

[3] D. Lazar, Chlorophyll *a* fluorescence induction, Biochim. Biophys. Acta 1412 (1999) 1–28.

[4] C. Neubauer, U. Schreiber, The polyphasic rise of chlorophyll fluorescence upon onset of strong continuous illumination: I. Saturation characteristics and partial control by the Photosystem II acceptor side, Z. Naturforsch. 42c (1987) 1246–1254.

[5] U. Schreiber, C. Neubauer, The polyphasic rise of chlorophyll fluorescence upon onset of continuous illumination: II. Partial control by the Photosystem II donor side and possible ways of interpretation, Z. Naturforsch. 42c (1987) 1255–1264.

[6] R.J. Strasser, A. Srivastava, Govindjee, Polyphasic chlorophyll *a* fluorescence transient in plants and cyanobacteria, Photochem. Photobiol. 61 (1995) 32–42.

[7] G. Samson, O. Prasil, B. Yaakoubd, Photochemical and thermal phases of chlorophyll *a* fluorescence, Photosynthetica 37 (1999) 163–182.

[8] P. Pospisil, H. Dau, Chlorophyll fluorescence transients of Photosystem II membrane particles as a tool for studying photosynthetic oxygen evolution, Photosynth. Res. 65 (2000) 41–52.

[9] R. Delosme, Etude de l'induction de fluorescence des algues vertes et des chloroplastes au début d'une illumination intense, Biochim. Biophys. Acta 143 (1967) 108–128.

[10] J. Cao, Govindjee, Chlorophyll *a* fluorescence transient as an indicator of active and inactive Photosystem II in thylakoid membranes, Biochim. Biophys. Acta 1015 (1990) 180–188.

[11] G.H. Krause, E. Weis, Chlorophyll fluorescence and photosynthesis: the basics, Annu. Rev. Plant Physiol. Plant Mol. Biol. 42 (1991) 313–349.

[12] A. Srivastava, R.J. Strasser, Govindjee, Polyphasic rise of chlorophyll *a* fluorescence in herbicide-resistant D1 mutants of chlamydomonas reinhardtii, Photosynth. Res. 43 (1995) 131–141.

[13] C. Vernotte, A.L. Etienne, J.-M. Briantais, Quenching of the system II chlorophyll fluorescence by the plastoquinone pool, Biochim. Biophys. Acta 545 (1979) 519–527.

[14] J.-M. Briantais, C. Vernotte, M. Picaud, G.H. Krause, A quantitative study of the slow decline of chlorophyll *a* fluorescence in isolated chloroplasts, Biochim. Biophys. Acta 548 (1979) 128–138.

[15] Govindjee, Photosystem II heterogeneity: the acceptor side, Photosynth. Res. 25 (1990) 151–160.

[16] J. Lavergne, J.-M. Briantais, Photosystem II heterogeneity, in: D.R. Ort, C.F. Yocum (Eds.), Oxygenic Photosynthesis: The Light Reactions, Kluwer Academic, Dordrecht, 1996, pp. 265–287.

[17] P. Joliot, J. Lavergne, D. Beal, Plastoquinone compartmentation in chloroplasts: I. Evidence for domains with different rates of photoreduction, Biochim. Biophys. Acta 1101 (1992) 1–12.

[18] X. Barthélemy, R. Popovic, F. Franck, Studies on the O-J-I-P transient of chlorophyll fluorescence in relation to photosystem II assembly and heterogeneity in plastids of greening barley, J. Photochem. Photobiol., B Biol. 39 (1997) 213–218.

[19] P. Joliot, A. Joliot, B. Bouges, G. Barbieri, Studies of system II photocenters by comparative measurements of luminescence, fluorescence and oxygen emission, Photochem. Photobiol. 14 (1971) 287–305.

[20] B.D. Hsu, Evidence for the contribution of the S-state transitions of oxygen evolution to the initial phase of fluorescence induction, Photosynth. Res. 36 (1993) 81–88.

[21] I. Moya, Durée de vie et rendement de fluorescence de la chlorophylle in vivo. Leur relation dans différents modèles d'unités photosynthétiques, Biochim. Biophys. Acta 368 (1974) 214–227.

[22] S. Malkin, D. Wong, Govindjee, H. Merkelo, Parallel measurements on fluorescence life-time and intensity changes from leaves during the fluorescence induction, Photobiochem. Photobiophys. 1 (1980) 83–89.

[23] A.R. Holzwarth, J. Wendler, W. Haehnel, Time-resolved picosecond fluorescence spectra of the antenna chlorophylls in *Chlorella vulgaris*. Resolution of Photosystem I fluorescence, Biochim. Biophys. Acta 807 (1985) 155–167.

[24] M. Hodges, I. Moya, Time-resolved chlorophyll fluorescence studies of photosynthetic membranes: resolution and characterisation of four kinetic components, Biochim. Biophys. Acta 849 (1986) 193–202.

[25] I. Moya, P. Sebban, W. Haehnel, Lifetime of excited states and quantum yield of chlorophyll *a* fluorescence in vivo, in: Govindjee, J. Amesz, D.C. Fork (Eds.), Light Emission By Plants and Bacteria, Academic Press, Orlando, FL, 1986, pp. 161–190.

[26] T.A. Roelofs, C.-H. Lee, A.R. Holzwarth, Global target analysis of picosecond chlorophyll fluorescence kinetics from pea chloroplasts. A new approach to the characterisation of the primary processes in photosystem II α- and β-units, Biophys. J. 61 (1992) 1147–1163.

[27] J.-M. Briantais, J. Dacosta, Y. Goulas, J.-M. Ducruet, I. Moya, Heat-stress induces in leaves an increase of the minimum level of chlorophyll fluorescence, F_o: a time resolved analysis, Photosynth. Res. 46 (1996) 189–196.

[28] S. Vasil'ev, D. Bruce, Nonphotochemical quenching of excitation energy in photosystem II. A picosecond time-resolved study of the low yield of chlorophyll *a* fluorescence induced by single-turnover flash in isolated spinach thylakoids, Biochemistry 37 (1998) 11046–11054.

[29] H. Dau, Molecular mechanisms and quantitative models of variable photosystem II fluorescence, Photochem. Photobiol. 60 (1994) 1–23.

[30] J. Flexas, J.-M. Briantais, Z.G. Cerovic, H. Medrano, I. Moya, Steady-state and maximum chlorophyll fluorescence responses to water stress in grapevine leaves: a new remote sensing system, Remote Sens. Environ. 73 (2000) 283–297.

[31] R.D. Spencer, G. Weber, Measurements of subnanosecond fluorescence lifetimes with a cross-correlation phase fluorometer, Ann. N.Y. Acad. Sci. 158 (1969) 361–376.

[32] L. Camenen, Y. Goulas, G. Guyot, Z.G. Cerovic, G. Schmuck, I. Moya, Estimation of the chlorophyll fluorescence lifetime of plant canopies: validation of a deconvolution method based on the use of a 3-D canopy mockup, Remote Sens. Environ. 57 (1996) 79–87.

[33] F. Morales, N. Moise, R. Quilez, A. Abadia, J. Abadia, I. Moya, Iron deficiency interrupts energy transfer from a disconnected part of the antenna to the rest of Photosystem II, Photosynth. Res. 70 (2001) 207–220.

[34] A. Krieger-Liszkay, A.W. Rutherford, Influence of herbicide binding on the redox potential of the quinone acceptor in Photosystem II: relevance to photodamage and phytotoxicity, Biochemistry 37 (1998) 17339–17344.

[35] A.L. Etienne, J. Lavergne, Action du m-dinitrobenzene sur la phase thermique d'induction de fluorescence en photosynthèse, Biochim. Biophys. Acta 283 (1972) 268–278.

[36] R. Croce, G. Zucchelli, F.M. Garlaschi, R. Bassi, R.C. Jennings, Excited state equilibration in the Photosystem I–light-harvesting I complex: P700 is almost isoenergetic with its antenna, Biochemistry 35 (1996) 8572–8579.

[37] S. Apostol, J.-M. Briantais, N. Moise, Z.G. Cerovic, I. Moya, Photoinactivation of the photosynthetic electron transport chain by accumulation of over-saturating light pulses given to dark-adapted pea leaves, Photosynth. Res. 67 (2001) 215–227.

[38] E. Pfundel, Estimating the contribution of Photosystem I to total leaf chlorophyll fluorescence, Photosynth. Res. 56 (1998) 185–195.

[39] G. Schmuck, I. Moya, Time-resolved chlorophyll fluorescence spectra of intact leaves, Remote Sens. Environ. 47 (1994) 72–76.

[40] G. Agati, Z.G. Cerovic, I. Moya, The effect of decreasing temperature up to chilling values on the in vivo F685/F735 chlorophyll fluorescence ratio in *Phaseolus vulgaris* and *Pisum sativum*: the role of the Photosystem I contribution to the 735 nm fluorescence band, Photochem. Photobiol. 72 (2000) 75–84.

[41] B. Genty, J. Wonders, N.R. Baker, Non-photochemical quenching of F_o in leaves is emission wavelength dependent: consequences for quenching analysis and its interpretation, Photosynth. Res. 26 (1990) 133–139.

[42] U. Schreiber, W. Vidaver, Rapid light-induced changes of energy distribution between photosystem I and II, FEBS Lett. 62 (1976) 194–197.

[43] U. Schreiber, W. Vidaver, The I-D fluorescence transient. An indicator of rapid energy distribution changes in photosynthesis, Biochim. Biophys. Acta 440 (1976) 205–214.

[44] U. Schreiber, R. Fink, W. Vidaver, Fluorescence induction in whole leaves: differentiation between the two leaf sides and adaptation to different light regimes, Planta 133 (1977) 121–129.

[45] N.E. Geacintov, J. Breton, Energy transfer and fluorescence mechanisms in photosynthetic membranes, CRC Crit. Rev. Plant Sci. 5 (1987) 1–44.

[46] L.A. Tumerman, E.M. Sorokin, Fotosinteticheskaya edinitsa: "fizicheskaya" ili "statisticheskaya" model? (The photosynthetic unit: a "physical" or "statistical" model?), Mol. Biol. 1 (1967) 628–638.

[47] J.-M. Briantais, H. Merkelo, Govindjee, Lifetime of the excited state (τ) in vivo: III. Chlorophyll during fluorescence induction in *Chlorella pyrenoidosa*, Photosynthetica 6 (1972) 133–141.

[48] M. Hodges, I. Moya, Modification of room-temperature picosecond chlorophyll fluorescence kinetics in Photosystem-II-enriched particles by photochemistry, Biochim. Biophys. Acta 892 (1987) 42–47.

[49] M. Hodges, I. Moya, Time-resolved chlorophyll fluorescence studies on pigment–protein complexes from photosynthetic membranes, Biochim. Biophys. Acta 935 (1988) 41–52.

[50] W. Haehnel, J.A. Nairn, P. Reisberg, K. Sauer, Picosecond fluorescence kinetics and energy transfer in chloroplasts and algae, Biochim. Biophys. Acta 680 (1982) 161–173.

[51] T.C. Vogelmann, J.R. Evans, Profiles of light absorption and chlorophyll within spinach leaves from chlorophyll fluorescence, Plant Cell Environ. 25 (2002) 1313–1323.

[52] S. Malkin, P.A. Armond, H.A. Mooney, D.C. Fork, Photosystem II photosynthetic unit sizes from fluorescence induction in leaves, Plant Physiol. 67 (1981) 570–579.

[53] W.L. Butler, R.J. Strasser, Does the rate of cooling affect fluorescence properties of chloroplasts at − 196 °C, Biochim. Biophys. Acta 462 (1977) 283–289.

[54] F. Terjung, Reabsorption of chlorophyll fluorescence and its effects on the spectral distribution and the picosecond decay of higher plant leaves, Z. Naturforsch., C 53 (1998) 924–926.

[55] W.L. Butler, Energy distribution in the photochemical apparatus of photosynthesis, Annu. Rev. Plant Physiol. 29 (1978) 345–378.

[56] A.M. Gilmore, T.L. Hazlett, P.G. Debrunner, Govindjee, Photosystem II chlorophyll *a* fluorescence lifetimes and intensity are independent of the antenna size differences between barley wild-type and chlorina mutants: photochemical quenching and xanthophyll cycle-dependent nonphotochemical quenching of fluorescence, Photosynth. Res. 48 (1996) 171–187.

[57] H.J. van Gorkom, J.J. Tamminga, J. Haveman, Primary reactions, plastoquinone and fluorescence yield in subchloroplast fragments prepared with deoxycholate, Biochim. Biophys. Acta 347 (1974) 417–438.

[58] A.P.G.M. Thielen, H.J. van Gorkom, Redox potentials of electron acceptors in photosystem II_α and II_β, FEBS Lett. 129 (1981) 205–209.

[59] B.D. Hsu, J.Y. Lee, Fluorescence quenching by plastoquinone in an oxygen-evolving photosystem-II-enriched preparation, J. Photochem. Photobiol., B Biol. 30 (1995) 57–61.

[60] D.M. Kramer, G. DiMarco, F. Loreto, Contribution of plastoquinone quenching to saturation pulse-induced rise of chlorophyll fluorescence in leaves, in: P. Mathis (Ed.), Photosynthesis: from Light to Biosphere, vol. I, Kluwer Academic, Dordrecht, 1995, pp. 147–150.

[61] I. Moya, Application de la fluorimétrie de phase a l'étude de la durée de vie et du rendement de la fluorescence de la chlorophylle in vivo, PhD Thesis, Université de Paris XI, Orsay, 1979.

[62] J. Maroc, J. Garnier, Studies of cytochrome *b*-563 and P700 in three non-photosynthetic mutants of *Chlamydomonas reinhardtii*, Biochim. Biophys. Acta 292 (1973) 477–490.

[63] Y. Goulas, Teledétection de la fluorescence des couverts végétaux: Temps de vie de la fluorescence chlorophyllienne et fluorescence bleue, PhD Thesis, Université de Paris XI, Orsay, 1992.

[64] B. Genty, Y. Goulas, B. Dimon, G. Peltier, J.-M. Briantais, I. Moya, Modulation of efficiency of primary conversion in leaves, mechanisms involved at PS2, in: N. Murata (Ed.), Research in Photosynthesis, Kluwer Academic, Dordrecht, The Nedherlands, 1992, pp. 603–610.

[65] M.R. Eftink, Fluorescence quenching: theory and applications, in: J.R. Lakowicz (Ed.), Topics in Fluorescence Spectroscopy, Principles, vol. 2, Plenum, New York, 1991, pp. 53–126.

[66] J. Kurreck, R. Schodel, G. Renger, Investigation of the plastoquinone pool size and fluorescence quenching in thylakoid membranes and Photosystem II (PS II) membrane fragments, Photosynth. Res. 63 (2000) 171–182.

[67] J. Lavergne, P. Joliot, Restricted diffusion in photosynthetic membranes, Trends Biochem. Sci. 16 (1991) 129–134.

[68] J. Lavergne, J.-P. Bouchaud, P. Joliot, Plastoquinone compartmentation in chloroplasts: II. Theoretical aspects, Biochim. Biophys. Acta 1101 (1992) 13–22.

[69] M. Bradbury, N.R. Baker, Analysis of the induction of chlorophyll

fluorescence in leaves and isolated thylakoids: contributions of photochemical and non-photochemical quenching, Proc. R. Soc. Lond. B 220 (1983) 251–264.

[70] B. Bossmann, J. Knoetzel, S. Jansson, Screening of *chlorina* mutants of barley (*Hordeum vulgare* L.) with antibodies against light-harvesting proteins of PS I and PS II: absence of specific antenna proteins, Photosynth. Res. 52 (1997) 127–136.

[71] J.R. Andrews, M.J. Fryer, N.R. Baker, Consequences of LHC II deficiency for photosynthetic regulation in *chlorina* mutants of barley, Photosynth. Res. 44 (1995) 81–91.

[72] R. Bassi, F. Rigoni, G.M. Giacometti, Chlorophyll binding proteins with antenna function in higher plants and green algae, Photochem. Photobiol. 52 (1990) 1187–1206.

[73] S. Preiss, J.P. Thornber, Stability of the apoproteins of light-harvesting complex I and II during biogenesis of thylakoids in the chlorophyll *b*-less barley mutant *chlorina* f2, Plant Physiol. 107 (1995) 709–717.

[74] M. Krol, M.D. Spangfort, N.P.A. Hunner, G. Oquist, P. Gustafsson, S. Jansson, Chlorophyll *a*/*b*-binding proteins, pigment conversions, and early light-induced proteins in a chlorophyll *b*-less barley mutant, Plant Physiol. 107 (1995) 873–883.

[75] M. Krol, A.G. Ivanov, S. Jansson, K. Kloppstech, N.P.A. Hunner, Greening under high light or cold temperature affects the level of xanthophyll-cycle pigments, early light-inducible proteins, and light-harvesting polypeptides in wild-type barley and the *chlorina* f2 mutant, Plant Physiol. 120 (1999) 193–203.

[76] P. Horton, A.V. Ruban, D. Rees, G. Noctor, A.A. Pascal, A. Young, Control of the light harvesting function of chloroplast membranes by aggregation of the LHCII chlorophyll protein complex, FEBS Lett. 292 (1991) 1–4.

[77] C.W. Mullineaux, A.A. Pascal, P. Horton, A.R. Holzwarth, Excitation-energy quenching in aggregates of the LHC-II chlorophyll–protein complex—a time-resolved fluorescence study, Biochim. Biophys. Acta 1141 (1993) 23–28.

[78] R. Bassi, M. Silvestri, P. Dainese, I. Moya, G.M. Giacometti, Effects of a non-ionic detergent on the spectral properties and aggregation state of the light-harvesting chlorophyll *a*/*b* protein complex (LHCII), J. Photochem. Photobiol., B Biol. 9 (1991) 335–354.

[79] A. Boussac, M. Hodges, J.-M. Briantais, I. Moya, The quenching characteristics of potassium iridic chloride and their meaning for the origin of chlorophyll fluorescence components, Photosynth. Res. 20 (1989) 173–189.

[80] Y. Nishioku, M. Nakagawa, M. Tsuda, M. Terazima, A spectrally silent transformation in the photolysis of octopus rhodopsin: a protein conformational change without any accompanying change of the chromophore's absorption, Biophys. J. 80 (2001) 2922–2927.

[81] A.V. Ruban, F. Calkoen, S.L.S. Kwa, R. van Grondelle, P. Horton, J.P. Dekker, Characterisation of LHC II in the aggregated state by linear and circular dichroism spectroscopy, Biochim. Biophys. Acta 1321 (1997) 61–70.

[82] A.V. Ruban, A.J. Young, P. Horton, Induction of nonphotochemical energy dissipation and absorbance changes in leaves—evidence for changes in the state of the light-harvesting system of Photosystem-II in vivo, Plant Physiol. 102 (1993) 741–750.

[83] A.V. Ruban, P. Horton, Regulation of non-photochemical quenching of chlorophyll fluorescence in plants, Aust. J. Plant Physiol. 22 (1995) 221–230.

[84] P. Horton, A.V. Ruban, R.G. Walters, Regulation of light harvesting in green plants, Annu. Rev. Plant Physiol. Plant Mol. Biol. 47 (1996) 655–684.

[85] A.V. Ruban, P. Horton, The xanthophyll cycle modulates the kinetics of nonphotochemical energy dissipation in isolated light-harvesting complexes, intact chloroplasts, and leaves of spinach, Plant Physiol. 119 (1999) 531–542.

[86] I. Moya, P. Tapie, Lifetime studies by phase fluorometry in isolated light-harvesting complexes (LHC): dependence on the aggregation state, in: C. Sybesma (Ed.), Advances in Photosynthesis Research, vol. II, Martinus Nijhoff/Dr. W. Junk, The Hague, 1984, pp. 103–106.